Mutations in the voltage-gated potassium channel gene *KCNH1* cause Temple–Baraitser syndrome and epilepsy

Cas Simons[1#*], Lachlan D. Rash[1#], Joanna Crawford[1], Linlin Ma[1], Ben Cristofori-Armstrong[1], David Miller[1,2], Kelin Ru[1], Gregory J. Baillie[1], Yasemin Alanay[3], Adeline Jacquinet[4], François-Guillaume Debray[4], Alain Verloes[5,6], Joseph Shen[7], Gözde Yesil[8], Serhat Guler[8], Adnan Yuksel[8], John G. Cleary[9§], Sean M. Grimmond[1,2], Julie McGaughran[10,11], Glenn F. King[1*], Michael T. Gabbett[10,12*] and Ryan J. Taft[1,13,14*]

[1] Institute for Molecular Bioscience, The University of Queensland, Brisbane, QLD, Australia

[2] Wolfson Wohl Cancer Research Centre, Institute for Cancer Sciences, University of Glasgow, Garscube Estate, Switchback Road, Bearsden, Glasgow, Scotland G61 1BD, United Kingdom

[3] Pediatric Genetics, Department of Pediatrics, Acibadem University School of Medicine, Istanbul, Turkey

[4] Center for Human Genetics, CHU & University of Liège, Liège, Belgium

[5] Departement of Genetics, Assistance Publique des Hôpitaux de Paris (AP-HP), Robert Debré Hospital, Paris, France

[6] INSERM UMR 1141, Robert Debré Hospital, Paris, France

[7] Medical Genetics and Metabolism, Children's Hospital Central California, Madera, CA, USA

[8] Department of Medical Genetics, Bezmialem Vakif University School of Medicine, Istanbul, Turkey

[9] Real Time Genomics, Ltd., Hamilton, New Zealand.

[10] Genetic Health Queensland, Royal Brisbane & Women's Hospital, Brisbane, Australia

[11] School of Medicine, The University of Queensland, Brisbane, QLD, Australia

[12] School of Medicine, Griffith University, Gold Coast, QLD, Australia

[13] School of Medicine and Health Sciences, Departments of Integrated Systems Biology and of Pediatrics, George Washington University, Washington, DC, USA

[14] Illumina, Inc., San Diego, CA USA

[#] These Authors contributed equally to this work.

[*] These authors jointly directed this work.

[§] Deceased

To whom correspondence should be addressed:
CS: c.simons@imb.uq.edu.au
RJT: rtaft@illumina.com

Introductory Paragraph

Temple-Baraitser syndrome (TBS) is a multi-system developmental disorder characterized by intellectual disability, epilepsy and hypoplasia or aplasia of the nails of the thumb and great toe[1,2]. Here we report damaging *de novo* mutations in *KCNH1* (Ether-A-Go-Go, EAG1, K_V10.1), a voltage-gated potassium channel that is predominantly expressed in the central nervous system (CNS), in six TBS individuals. Characterization of these mutations in both Xenopus oocytes and human HEK293T cells revealed decreased threshold of activation and delayed deactivation, demonstrating that TBS-associated *KCNH1* mutations lead to deleterious gain-of-function. Consistent with this result, we find that two TBS mothers with epilepsy, but who are otherwise healthy, are low-level (10% and 27%) mosaic carriers of pathogenic *KCNH1* mutations. Consistent with recent reports[3-8], this demonstrates that the etiology of many unresolved central nervous systems disorders, including epilepsies, may be explained by pathogenic mosaic mutations.

Main text

TBS [MIM: 611816], which was first formally described in 1991, has a wide and severe phenotypic spectrum that includes intellectual disability, seizures, and dysmorphic features[1,2] (**Fig. 1**). TBS is rare, with only five cases reported to date, although it is possible that TBS is largely unrecognized by the clinical community and therefore under-reported[9]. The disease is sporadic in nature, and although a genetic etiology has been suspected[10], the lack of familial recurrence or defined cohorts has inhibited attempts to identify the genetic basis of the disease.

In this study we recruited six unrelated TBS individuals and their parents for analysis by whole exome sequencing (**Table 1** and **Supplementary Note**). This study was approved by the Royal Brisbane and Women's Hospital Human Research Ethics Committee, The Royal Children's Hospital Human Research Ethics Committee, and The University of Queensland Medical Research Ethics Committee. Informed consent was obtained from all study subjects. DNA was isolated from peripheral blood from all participants, and in select cases also from saliva and buccal cells. Exome sequencing and analysis was performed on all six probands and four sets of parents (Online Methods). A minimum of 19 Gb of sequence was generated for each individual, yielding a mean depth of 165-fold coverage and an average of 93% of target bases sequenced at ≥ 20X.

Given the severity of the TBS phenotype and its sporadic presentation, we first queried for pathogenic *de novo* mutations in the four cases for which exomes of the full family trio were sequenced (cases A-D). Using pedigree informed variant calling we filtered for candidates that were only detected in the proband, computationally predicted to be damaging[11,12] and were absent from dbSNP 141, the 1000 Genomes Project and the NHLBI ESP6500 databases. This revealed that the TBS individuals carried missense *de novo* mutations in the voltage-gated potassium channel gene, *KCNH1* (MIM 603305; NM_172362; **Table 1; Fig. 2a**). Subsequent investigation of the two proband-only exomes (cases E and F) also revealed damaging *KCNH1* missense variants, which were similarly absent from all public variant databases and shown to

be *de novo* by targeted Sanger sequencing of both parents (**Table 1**). All TBS-associated *KCNH1* mutations were absent from an in-house control exome dataset from more than 100 family trios of children with neurological disorders.

Evaluation of the TBS family case histories revealed that the mothers of two subjects (A.1 and B.1) had been previously diagnosed with epilepsy but presented with no other phenotypic features suggestive of TBS (**Table 1** and **Supplementary Note**). In light of recent reports of pathogenic mosaicism in a range of neurological disorders[3-8], this suggested the potential for low-level *KCNH1* mutation mosaicism in these individuals. Directed reanalysis of exome sequence reads revealed that although both A.1 and B.1 had *KCNH1* genotype calls of "homozygous wild type" at the sites of mutation, a small proportion of reads supported the disease allele associated with their children and was not observed in the subjects' fathers (**Table 1**).

To confirm maternal mosaicism we performed targeted high-depth sequencing of *KCNH1* exon eight and obtained more than 40,000-fold coverage for each sample (**Supplementary Table 2**). In subject A.1 the NM_172362.2:c.1508A>G variant was confirmed at very low, but detectable, levels: 4.7% of reads from two independently drawn blood samples, and 3.4% and 4.5% of reads from fibroblast and saliva samples, respectively (**Supplementary Table 2**). In B.1 the NM_172362.2:c.1465C>T mutation was detected in 13.6% of reads from targeted reanalysis of DNA from peripheral blood (**Supplementary Table 2**).

KCNH1 is a highly conserved member of the EAG subfamily of voltage-gated potassium channels. It is predominantly expressed in the adult CNS, but restricted cell populations expressing KCNH1 have been identified throughout the human body[13]. *KCNH1* is expressed in ~70% of solid tumors[14] and inhibition of KCNH1 activity has been shown to restrict cancer cell proliferation[15]. Relatively little is known about the normal physiological function of KCNH1. It has, however, been identified as a regulator of cell proliferation in bone marrow derived mesenchymal stem cells[16], and its activity appears to be cell-cycle regulated[17], suggesting that it is likely to be involved in fundamental cellular and developmental processes. Indeed, *KCNH1* is predicted to be in the 7th percentile of genes intolerant to functional genetic variation[18].

KCNH1 channels are homotetramers, with each subunit composed of six transmembrane helices flanked by cytoplasmic C-terminal and N-terminal domains (**Fig. 2b**). Remarkably, three of the TBS subjects carry the same *de novo* heterozygous missense mutation (NM_172362.2:c.1480A>G, p.Ile494Val), and two other subjects have *de novo* mutations within 30 bp of this mutation (NM_172362.2:c.1508A>G, p.Gln503Arg; NM_172362.2:c.1465C>T, p.Leu489Phe). These mutations all occur within exon eight and affect residues located in the S6 transmembrane helix, which is a central component of the channel pore[19] (**Fig. 2b**). The *de novo* mutation identified in the final subject lies in exon six (NM_172362.2:c.651G>C, p.Lys217Asn) and is located near the boundary between the N-terminal cytoplasmic domain and the S1 transmembrane helix (**Fig. 2b**). All four affected residues are highly conserved across the *KCNH* gene family (**Fig. 2c**).

To determine the effect of these mutations on the biophysical properties of KCNH1, all four mutant channels were expressed in *Xenopus laevis* oocytes and Human Embryonic Kidney

293T (HEK293T) cells and investigated using two-electrode voltage clamp or patch-clamp electrophysiology, respectively. Activation of wild-type or mutant KCNH1 expressed in oocytes or HEK293T cells resulted in robust voltage-dependent outward currents, consistent with the expression of functional membrane-bound potassium channels (**Fig. 3a,b** and **Supplementary Fig. 1a,b**). In both systems, however, each of the four mutations showed a pronounced decrease in threshold of activation when compared to wild-type KCNH1 (**Fig. 3c** and **Supplementary Fig. 1c**). For example, in HEK293T cells, the voltage of half maximal activation ($V_{1/2}$) of wild-type KCNH1 channels was 20.2 mV. In contrast, the $V_{1/2}$ for all four mutant channels was negatively shifted by at least 33 mV compared to the wild-type channel, with values between –13.7 mV and –28.9 mV (**Table 2**). Deactivation was also profoundly affected, with all mutant channels closing more slowly than the wild-type (**Fig. 3d** and **Supplementary Fig. 1d**). These data indicate that all four *de novo KCNH1* mutations identified in this study lead to gain-of-function.

Taken together, these results demonstrate that mutations in KCNH1 can lead to deleterious channel activity and cause TBS. Furthermore, the phenotypic separation between two of the TBS patients and their mothers, who only suffer from epilepsy, may be the result of reduced mutational burden in the mosaic mothers. These findings are in contrast to studies of *KCNH1* knockout mice, which are viable and show phenotypic abnormalities limited to mild hyperactivity and sensitivity to haloperidol-induced catalepsy[20]. This suggests that *KCNH1* loss-of-function mutations may be relatively well tolerated, but those resulting in aberrant channel activity are likely to be pathogenic.

A wide range of genetic disorders have been associated with potassium channel mutations including at least thirteen forms of epilepsy[21-23], several ataxias[24,25] and a form of inherited deafness[26]. Developmental phenotypes associated with potassium channelopathies are less common, but not unprecedented. For example, Andersen-Tawil syndrome (MIM 170390), an autosomal dominant disorder resulting from mutations in KCNJ2, presents with distinctive dysmorphic features including scoliosis, low-set ears, wide-set eyes, small chin, and broad forehead[27]. We propose that both the CNS and developmental defects observed in TBS subjects result from hyperactive *KCNH1*, which disrupts both cell proliferation (or migration) and neuronal activity.

Although many epilepsies are believed to have a genetic basis, a definitive diagnosis can only be provided in a minority of cases[28]. There is, however, a growing body of evidence indicating that genetic mosaicism is an important factor in the etiology of many neurological disorders[29]. For example, there have been several reports of epilepsy resulting from mosaic mutations in the ion channels SCN1A[3-5] and KCNQ2[6,7], and a recent systematic investigation has found that mosaic mutations are frequent in patients with brain malformations[8]. Our results indicate that low level mosaicism in *KCNH1* may also contribute to epilepsy, and together with the previously reported cases, highlights the need to develop novel informatic approaches to identify pathogenic mosaic variants in large-scale and diagnostic sequencing efforts.

Figures

Figure 1. Phenotypic features of Temple-Baraitser Syndrome. (a) Facial features aged 2½ years and (b) 4 years. Note the myopathic facies, flat forehead, broad depressed nasal bridge, bilateral epicanthic folds, short columella, long shallow philtrum, and broad mouth with downturned corners. (c) Left hand (d) and left foot. Note broad adducted terminal thumb and nail hypoplasia of the thumb and nail aplasia of the great toe. (e) Radiographs of the left foot and (f) left hand. Note the radiolucencies in the distal phalanges. Consent to publish images of the subject was obtained. Images b-f reproduced with permission[2].

Figure 2. *KCNH1* mutations in subjects with Temple-Baraitser Syndrome. (a) Genomic structure of the *KCNH1* gene. The position of the TBS-associated *de novo* mutations are indicated in red. The transcription start site is shown as a blue arrow. (b) Schematic of the KCNH1 protein showing the six transmembrane helices (S1–S6), the intracellular N-terminal region containing an eag domain (EAG), and the C-terminal region containing a cyclic nucleotide binding homology domain (CNBHD). The locations of the TBS-associated *de novo* mutation sites are indicated by red stars. (c) Multiple sequence alignment of all eight human KCNH family proteins. The mutated KCNH1 residues are highlighted in bold. Conservation of residues across the gene family is indicated in red.

Figure 3. Mutant KCNH1 channels show increased voltage sensitivity and delayed deactivation. (a) Representative families of whole-cell currents elicited by steps from –120 mV to +120 mV in 10 mV increments in HEK293T cells expressing wild-type (WT) and mutant KCNH1 (holding potential of –120 mV). The arrowheads represent zero current. (b) Plot of mean current density versus test voltage for WT and TBS mutant KCNH1 channels expressed in HEK293T cells. (c) Activation current-voltage relationship (±s.e.m.) for WT, p.Lys217Asn, p.Leu489Phe, p.Ile494Val and p.Gln503Arg expressed in HEK293T cells. Currents were measured at the end of the activation test pulse. (d) Fast and slow time constants (τ) of deactivation for WT and mutant KCNH1 channels expressed in HEK293T cells, analyzed from the tail current at –140 mV following a maximally activating pre-pulse to +80 mV. Data are presented as mean ± s.e.m. with numbers of experiments indicated in parentheses. *P-values* calculated compared to WT using unpaired t-test with Welch's correction. * $P < 0.05$, ** $P < 0.01$.

Table 1: *KCNH1* genotypes from exome sequencing.

Family	Individual	Relationship	Condition	Genotype[1]	Wild-type reads	Alternative reads
A	A.0	Proband	TBS	c.1508A>G	90	71
	A.1	Mother	Epilepsy	-	144	6
	A.2	Father	-	-	142	0
B	B.0	Proband	TBS	c.1465C>T	75	81
	B.1	Mother	Epilepsy	-	102	8
	B.2	Father	-	-	177	0
C	C.0	Proband	TBS	c.1480A>G	73	96
	C.1	Mother	-	-	135	0
	C.2	Father	-	-	148	0
D	D.0	Proband	TBS	c.651G>C	37	37
	D.1	Mother	-	-	85	0
	D.2	Father	-	-	115	0
E	E.0	Proband	TBS	c.1480A>G	34	41
F	F.0	Proband	TBS	c.1480A>G	36	26

[1] Genotype of *KCNH1* (NM_172362) as called by rtgFamily variant caller.

Table 2: Voltage of half maximal activation values and slopes of the current-voltage relationships for WT and mutant KCNH1 channels.

	X. laevis oocytes				HEK293T cells			
	$V_{1/2}$	*P*	Slope	*P*	$V_{1/2}$	*P*	Slope	*P*
Wild-type	22.0±1.3	n.a.	19.7±1.1	n.a.	20.2±2.4	n.a.	17.0±0.9	n.a.
p.Lys217Asn	-18.0±1.7	**$5.2x10^{-10}$**	18.7±1.6	0.433	-20.0±2.3	**$1.3x10^{-11}$**	21.3±1.0	**0.004**
p.Leu489Phe	-23.5±1.4	**$7.4x10^{-15}$**	16.1±1.2	**0.011**	-16.2±3.8	**$9.2x10^{-7}$**	19.7±1.0	0.011
p.Ile494Val	-14.5±1.7	**$8.7x10^{-9}$**	17.6±1.5	0.371	-13.7±2.5	**$2.7x10^{-9}$**	21.1±1.1	0.064
p.Gln503Arg	-38.2±1.1	**$6.3x10^{-19}$**	17.9±1.0	0.852	-28.9±2.3	**$8.1x10^{-14}$**	19.3±0.7	0.052

$V_{1/2}$ and slope ± s.e.m. *P-values* calculated compared to WT using unpaired t-test with Welch's correction. Significant *P* values are shown in bold.

Online Methods

Exome and Amplicon sequencing

DNA library preparation and exome enrichment was performed using the Illumina Nextera Rapid Capture kit. Captured libraries were sequenced on an Illumina HiSeq 2000 according to the 2 x 100 bp paired-end read-sequencing protocol at the Queensland Centre for Medical Genomics. Reads were aligned to the reference human genome (GRCh37) and pedigree informed variant calling was performed using the Real Time Genomics (RTG) integrated analysis tool rtgFamily v3.2[30]. All variants were annotated using SnpEff v3.4[31]. Subsequent analysis and identification of candidate variants was performed with an in-house workflow incorporating the annotated variant data and pedigree information.

Exons 6 and 8 of *KCNH1* were PCR amplified with 60ºC annealing and a 1 min per kb extension time under Phusion Taq amplification conditions (see **Supplementary Table 3** for primer sequences). MiSeq libraries were prepared from 1 ng of PCR product using the Nextera XT library preparation kits and sequenced using the MiSeq 300 cycle v2 kits as previously described[32]. The first 50,000 reads from each sample were quality trimmed using trimmomatic[33], aligned to the reference human genome (GRCh37) using BWA-MEM[34] and variants were called with Varscan2[35].

DNA constructs

Plasmids (pUC57) containing the wild-type coding sequence of *KCNH1* isoform NM_002238 along with p.Gln476Arg and p.Ile467Val versions (equivalent to p.Gln503Arg and p.Ile494Val in *KCNH1* isoform NM_172362) were purchased from GenScript. Coding sequences were sub-cloned into the pEF6 mammalian expression vector with the addition of a C-terminal HA epitope tag. Site directed mutagenesis was used to introduce p.Lys217Asn and p.Leu462Phe variants (equivalent to p.Lys217Asn and p.Leu489Phe in *KCNH1* isoform NM_172362) into the wild-type construct.

Oocyte Electrophysiology

Channel function was assessed using two-electrode voltage-clamp experiments performed on *Xenopus laevis* oocytes expressing homomeric KCNH1 channels prepared as previously described[36]. wild-type and mutant KCNH1 cRNA was synthesized using an mMessage mMachine *in vitro* transcription kit (Ambion Inc., Austin, TX, USA) and injected at 4 ng per oocyte. Oocytes were incubated at 17°C in ND96 solution containing 96 mM NaCl, 2 mM KCl, 1.8 mM $CaCl_2$, 2 mM $MgCl_2$, 5 mM HEPES, 5 mM pyruvate, 50 µg/ml gentamicin (pH 7.4), and horse serum (2.5%). Experiments were performed at room temperature (21–22°C) in ND96 solution (as defined above, but minus serum, pyruvate and antibiotics) 1–2 days after cRNA injection. Oocytes were clamped at –100 mV (Axoclamp 900A) using electrodes of resistance 0.5–0.8 MΩ when filled with 3 M KCl solution. The bath was constantly perfused and 3 M KCl agar bridges were used to ground the bath. To test the voltage-dependent activation of KCNH1 channels, 2 s pulses from –120 mV to +80 mV in 20 mV steps were used to activate the

channel from holding potential of –100 mV, followed by a 1 s step to –110 mV with a 15 second pulse interval. The currents elicited by the test pulse were normalized to I_{max}, plotted against test voltage and fitted with Boltzmann equation. The deactivation of KCNH1 channels was studied by first activating the channel at +80 mV for 1000 ms, then deactivating the channel with steps from –120 mV to 0 mV for 1500 ms before returning to holding potential of –100 mV with a 30 second pulse interval. The kinetics of deactivation was analyzed by fitting the deactivation at –90 mV with a double exponential equation (Clampfit10) and the Tau values compared using an unpaired *t*-test with Welch's correction. Voltage-dependence of steady-state inactivation was studied using the double-pulse protocol reported previously[37]. A 10 s conditioning pulse increasing from –130 mV to +35 mV in 15 mV steps (Vpre) preceded an activating 4.5 s test pulse to +30 mV every 30 s (**Suppl Fig. 1b**). The current elicited by the test pulse was normalized to I_{max} and plotted against conditioning voltage. Data acquisition and analysis were performed using pCLAMP10 software (Molecular Devices). Significant difference is defined as $P < 0.05$ (unpaired *t*-test with Welch's correction). *n*-values represent experiments from individual oocytes taken from at least three different frogs.

HEK293T Patch clamp Electrophysiology

HEK293T cells (CRL-11268, American Type Culture Collection) were cultured in DMEM supplemented with 10% FBS and 1% penicillin-streptomycin. Cells were tested negative for mycoplasma. To carry out electrophysiology studies in mammalian cells, HEK293T cells were transiently transfected with 2 µg of plasmid DNA (1 µg for p.Leu462Phe mutant) using Lipofectamine 2000 (Life Technologies) according to the manufacturers instructions. Patch-clamp experiments were conducted 24h post transfection at room temperature in the whole-cell configuration using an Axon MultiClamp 700B patch-clamp amplifier and associated standard equipment (Molecular Devices). Cells were continuously superfused with bath solution containing 140 mM NaCl, 2.5 mM KCl, 2 mM $CaCl_2$, 1 mM $MgCl_2$, 8 mM glucose and 10 mM HEPES, adjusted to pH 7.4 with NaOH. Patch pipettes were pulled from borosilicate glass and typically had a resistance of 2-5 MΩ when filled with the standard pipette solution containing 70 mM KF, 60 mM KCl, 15 mM NaCl, 5 mM EGTA-Na, 5 mM HEPES, adjusted to pH 7.2 with NaOH. Series resistance did not exceed 5 MΩ and was 70-80% compensated. Acquired currents were filtered at 1 kHz, sampled at 10 kHz, collected and analyzed using Clampex 10.0 Software (Molecular Devices).

To test the voltage-dependent activation of KCNH1 channels, 1 s pulses from –120 mV to +120 mV in 10 mV steps were used to activate the channel from holding potential of –120 mV, followed by a 400 ms step to –100 mV. The currents elicited by the test pulse were normalized to I_{max}, plotted against the test voltage and fitted with Boltzmann equation. The deactivation of KCNH1 channels was studied by first activating the channel at +80 mV for 800 ms, then deactivating the channel with steps from –140 mV to 0 mV for 500 ms before returning to holding potential of –120 mV. The kinetics of deactivation were analyzed by fitting the deactivation sweep at –140 mV with double exponential equation (Clampfit10) and the Tau values compared using an unpaired *t*-test with Welch's correction.

Author Contributions

C.S., R.J.T., M.T.G and J.M. conceived and designed the project. M.T.G., J.M., Y.A., A.J., F.D., A.V., J.S., G.Y., S.G. and A.Y. phenotyped the cases, provided clinical samples and provided clinical information. D.M. and S.M.G. were responsible for exome sequencing. C.S. performed all exome and variant analysis, with input from R.J.T. J.G.C. provided software and advice for sequence analysis. J.C., B.CA. and K.R. performed Sanger sequencing and constructed the expression vectors. L.D.R., L.M. and G.F.K. conceived the electrophysiology experiments, which were performed by L.D.R., B.CA. and L.M. J.C. prepared samples for targeted amplicon sequencing. Amplicon data analysis was performed by C.S. and G.J.B. All data was reviewed and synthesized by C.S. and R.J.T. The manuscript was drafted by C.S. and R.J.T. with input from M.G. and L.D.R. All authors discussed the results and commented on the manuscript.

Acknowledgements

We would like to thank the patients and their families for their participation in this study. Computational support was provided by the NeCTAR Genomics Virtual Laboratory and QRIScloud programs. We thank the QCMG and IMB sequencing facility teams for their assistance with this project and to Prof. Joe Lynch for providing access to his patch-clamp facilities. We also wish to thank Prof. Jamie Vandenberg for his helpful discussion of results. R.J.T. was supported by an Australian Research Council Discovery Early Career Research Award. L.M. is supported by NHMRC CJ Martin fellowship. This work was supported in part by a University of Queensland Foundation Research Excellence Award and a donation by J. & G.J. Crawford.

Competing financial interests

R.J.T. became an employee of Illumina, Inc. during the course of this project.

References

1. Temple, I. K. & Baraitser, M. Severe mental retardation and absent nails of hallux and pollex. *Am. J. Med. Genet.* **41,** 173–175 (1991).
2. Gabbett, M. T., Clark, R. C. & McGaughran, J. M. A second case of severe mental retardation and absent nails of hallux and pollex (Temple-Baraitser syndrome). *Am. J. Med. Genet.* **146A,** 450–452 (2008).
3. Depienne, C. *et al.* Mechanisms for variable expressivity of inherited SCN1A mutations causing Dravet syndrome. *Journal of Medical Genetics* **47,** 404–410 (2010).
4. Marini, C., Mei, D., Helen Cross, J. & Guerrini, R. Mosaic SCN1A mutation in familial severe myoclonic epilepsy of infancy. *Epilepsia* **47,** 1737–1740 (2006).
5. Selmer, K. K. *et al.* Parental SCN1A mutation mosaicism in familial Dravet syndrome. *Clin. Genet.* **76,** 398–403 (2009).
6. Kato, M. *et al.* Clinical spectrum of early onset epileptic encephalopathies caused by KCNQ2 mutation. *Epilepsia* **54,** 1282–1287 (2013).
7. Weckhuysen, S. *et al.* KCNQ2 encephalopathy: emerging phenotype of a neonatal epileptic encephalopathy. *Ann Neurol.* **71,** 15–25 (2012).
8. Jamuar, S. S. *et al.* Somatic mutations in cerebral cortical malformations. *N Engl J Med* **371,** 733–743 (2014).
9. Yesil, G., Guler, S., Yuksel, A. & Alanay, Y. Report of a patient with Temple-Baraitser syndrome. *Am. J. Med. Genet.* **164A,** 848–851 (2014).
10. Jacquinet, A. *et al.* Temple-Baraitser syndrome: a rare and possibly unrecognized condition. *Am. J. Med. Genet.* **152A,** 2322–2326 (2010).
11. Adzhubei, I. A. *et al.* A method and server for predicting damaging missense mutations. *Nat. Methods* **7,** 248–249 (2010).
12. Kumar, P., Henikoff, S. & Ng, P. C. Predicting the effects of coding non-synonymous variants on protein function using the SIFT algorithm. *Nat Protoc* **4,** 1073–1081 (2009).
13. Hemmerlein, B. *et al.* Overexpression of Eag1 potassium channels in clinical tumours. *Mol. Cancer* **5,** 41 (2006).
14. Urrego, D., Tomczak, A. P., Zahed, F., Stühmer, W. & Pardo, L. A. Potassium channels in cell cycle and cell proliferation. *Philos. Trans. R. Soc. Lond., B, Biol. Sci.* **369,** 20130094–20130094 (2014).
15. Gómez-Varela, D. *et al.* Monoclonal antibody blockade of the human Eag1 potassium channel function exerts antitumor activity. *Cancer Res.* **67,** 7343–7349 (2007).
16. Zhang, J. *et al.* Regulation of cell proliferation of human induced pluripotent stem cell-derived mesenchymal stem cells via ether-à-go-go 1 (hEAG1) potassium channel. *Am. J. Physiol., Cell Physiol.* **303,** C115–25 (2012).
17. Ouadid-Ahidouch, H. & Le Bourhis, X. Changes in the K+ current-density of MCF-7 cells during progression through the cell cycle: possible involvement of a h-ether. a-gogo K+ channel. *Recept. Channels* (2000).
18. Petrovski, S., Wang, Q., Heinzen, E. L., Allen, A. S. & Goldstein, D. B. Genic intolerance to functional variation and the interpretation of personal genomes. *PLoS Genet.* **9,** e1003709 (2013).
19. Tian, C. *et al.* Potassium channels: structures, diseases, and modulators. *Chem Biol Drug Des* **83,** 1–26 (2014).
20. Ufartes, R. *et al.* Behavioural and functional characterization of Kv10.1 (Eag1) knockout mice. *Hum. Mol. Genet.* **22,** 2247–2262 (2013).
21. D'Adamo, M. C., Catacuzzeno, L., Di Giovanni, G., Franciolini, F. & Pessia, M. K(+) channelepsy: progress in the neurobiology of potassium channels and epilepsy. *Front Cell Neurosci* **7,** 134 (2013).

22. Barcia, G. *et al.* De novo gain-of-function KCNT1 channel mutations cause malignant migrating partial seizures of infancy. *Nat. Genet.* **44,** 1255–1259 (2012).
23. Heron, S. E. *et al.* Missense mutations in the sodium-gated potassium channel gene KCNT1 cause severe autosomal dominant nocturnal frontal lobe epilepsy. *Nat. Genet.* **44,** 1188–1190 (2012).
24. Browne, D. L. *et al.* Episodic ataxia/myokymia syndrome is associated with point mutations in the human potassium channel gene, KCNA1. *Nat. Genet.* **8,** 136–140 (1994).
25. Lee, Y.-C. *et al.* Mutations in KCND3 cause spinocerebellar ataxia type 22. *Ann Neurol.* **72,** 859–869 (2012).
26. Coucke, P. J. *et al.* Mutations in the KCNQ4 gene are responsible for autosomal dominant deafness in four DFNA2 families. *Hum. Mol. Genet.* **8,** 1321–1328 (1999).
27. Tawil, R. *et al.* Andersen's syndrome: potassium-sensitive periodic paralysis, ventricular ectopy, and dysmorphic features. *Ann Neurol.* **35,** 326–330 (1994).
28. Epi4K Consortium *et al.* De novo mutations in epileptic encephalopathies. *Nature* **501,** 217–221 (2013).
29. Poduri, A., Evrony, G. D., Cai, X. & Walsh, C. A. Somatic mutation, genomic variation, and neurological disease. *Science* **341,** 1237758–1237758 (2013).
30. Cleary, J. G. *et al.* Joint variant and de novo mutation identification on pedigrees from high-throughput sequencing data. *J. Comput. Biol.* **21,** 405–419 (2014).
31. Cingolani, P. *et al.* A program for annotating and predicting the effects of single nucleotide polymorphisms, SnpEff: SNPs in the genome of Drosophila melanogaster strain w1118; iso-2; iso-3. *Fly (Austin)* **6,** 80–92 (2012).
32. Simons, C. *et al.* A De Novo Mutation in the β-Tubulin Gene TUBB4A Results in the Leukoencephalopathy Hypomyelination with Atrophy of the Basal Ganglia and Cerebellum. *Am. J. Hum. Genet.* **92,** 767–773 (2013).
33. Bolger, A. M., Lohse, M. & Usadel, B. Trimmomatic: a flexible trimmer for Illumina sequence data. btu170 (2014). doi:10.1093/bioinformatics/btu170
34. Li, H. & Durbin, R. Fast and accurate short read alignment with Burrows-Wheeler transform. *Bioinformatics* **25,** 1754–1760 (2009).
35. Koboldt, D. C. *et al.* VarScan 2: Somatic mutation and copy number alteration discovery in cancer by exome sequencing. *Genome Res.* **22,** 568–576 (2012).
36. Schroeder, C. I. *et al.* Chemical synthesis, 3D structure, and ASIC binding site of the toxin mambalgin-2. *Angew. Chem. Int. Ed. Engl.* **53,** 1017–1020 (2014).
37. Garg, V., Sachse, F. B. & Sanguinetti, M. C. Tuning of EAG K(+) channel inactivation: molecular determinants of amplification by mutations and a small molecule. *J. Gen. Physiol.* **140,** 307–324 (2012).

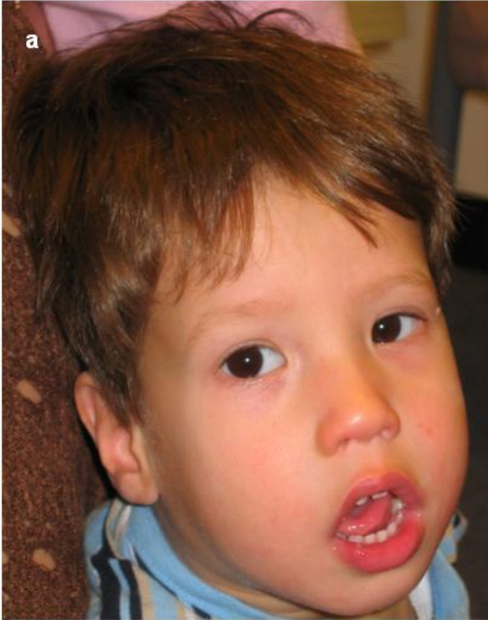
a
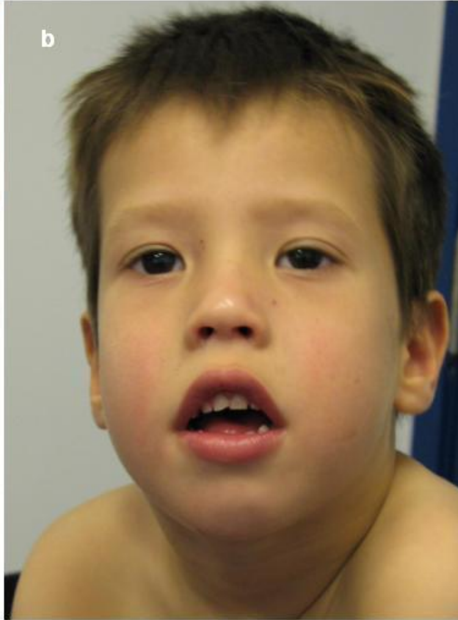
b
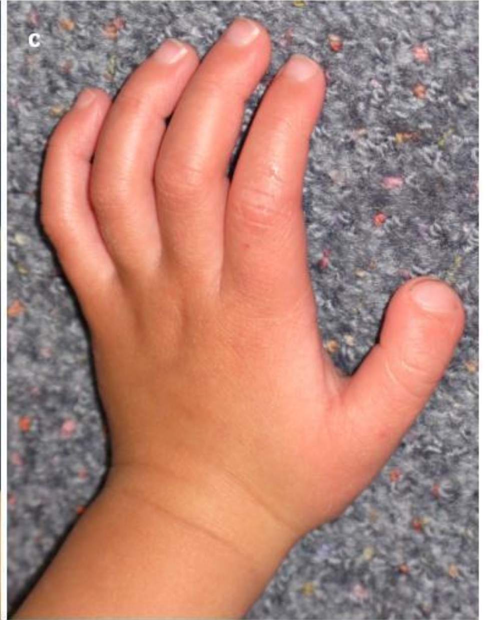
c
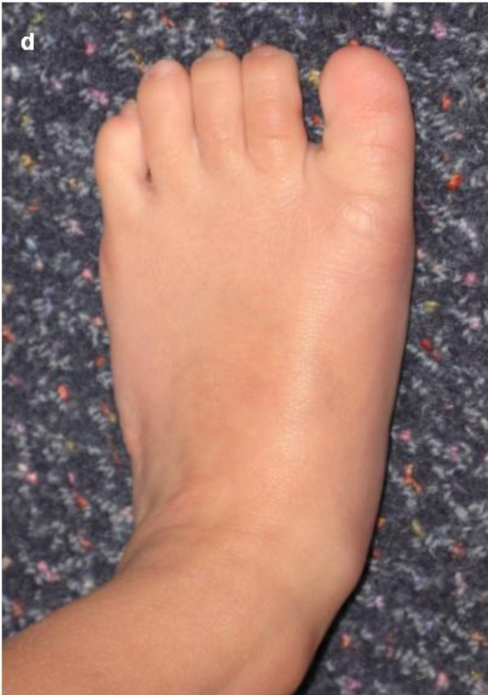
d
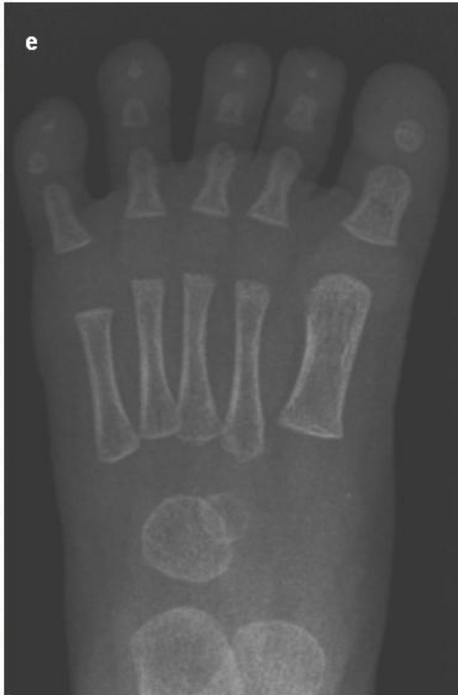
e
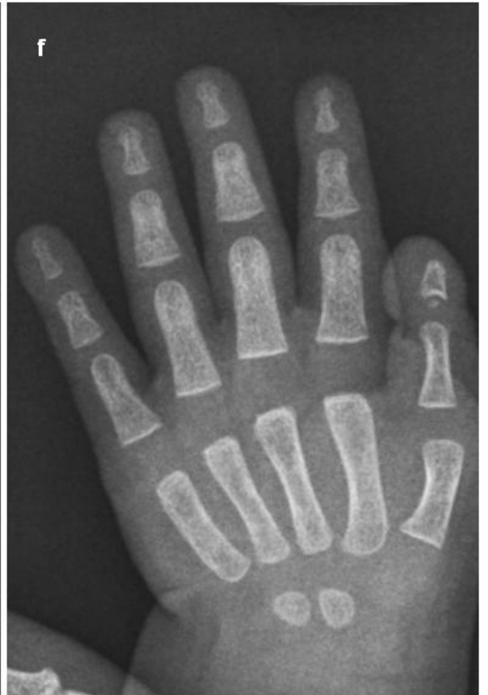
f

a

200kb

c.651G>C (p.K217N)

c.1465C>T (p.L489F)
c.1480A>G (p.I494V)
c.1508A>G (p.Q503R)

b

S1 S2 S3 S4 S5 S6

L489F
I494V
Q503R
K217N

COOH CNBHD

EAG NH2

c

```
KCNH1 LPQYKQEAPKTPPHIILHYCVFKTTWDWIILILTFYTAI 233
KCNH5 LPQYKQEAPKTPPHIILHYCAFKTTWDWVILILTFYTAI 172
KCNH2 LPEYKLQAPRIHRWTILHYSPFKAVWDWLILLLVIYTAV 83
KCNH7 LPEYKLQTPRINKFTILHYSPFKAVWDWLILLLVIYTAI 416
KCNH6 LPEYKLQAPRIHRWTILHYSPFKAVWDWLILLLVIYTAV 272
KCNH4 VPEYKVASVGGSRCLLLHYSVSKAIWDGLILLATFYVAV 242
KCNH3 LPEYKVAAIRKSPFILLHCGALRATWDGFILLATLYVAV 240
KCNH8 FPEYKVSDAKKSKFILLHFSTFKAGWDWLILLATFYVAV 237
      .*:**          :**    :: ** .**: .:*.*:

KCNH1 IFAVAIMMIGSLLYATIFGNVTTIFQQMYANTNRYHEML 516
KCNH5 MFSVAMMMVGSLLYATIFGNVTTIFQQMYANTNRYHEML 427
KCNH2 IFSICVMLIGSLMYASIFGNVSAIIQRLYSGTARYHTQM 337
KCNH7 IFSICVMLIGSLMYASIFGNVSAIIQRLYSGTARYHMQM 673
KCNH6 VFSICVMLIGSLMYASIFGNVSAIIQRLYSGTARYHTQM 476
KCNH4 IFSICTMLIGALMHAVVFGNVTAIIQRMYSRRSLYHSRM 492
KCNH3 IFSICTMLIGALMHAVVFGNVTAIIQRMYARRFLYHSRT 518
KCNH8 IFSICTMLIGALMHALVFGNVTAIIQRMYSRWSLYHTRT 487
      :*::. *::*:*::* :****::*:*::*:    **
```

a

Control

+120 mV

-120 mV

-100 mV

1 nA

100 ms

WT

2 nA

100 ms

K217N

4 nA

100 ms

L489F

2 nA

100 ms

I494V

2 nA

100 ms

Q503R

2 nA

100 ms